

# Aeroelastic Optimization of Wing Structure Using Curvilinear Spars and Ribs (SpaRibs)

Joe Robinson<sup>1</sup>, Steven Doyle<sup>1</sup>, Grant Ogawa<sup>1</sup>, and Myles Baker<sup>2</sup>

*M4 Engineering, Inc., Long Beach, California 90807*

Shuvodeep De<sup>3</sup>, Mohamed Jrad<sup>4</sup>, and Rakesh Kapania<sup>5</sup>

*Virginia Polytechnic Institute and State University, Blacksburg, VA, 24061-0203*

*and*

Chan-Gi Pak<sup>6</sup>

*NASA Armstrong Flight Research Center, Edwards, CA 93523-0273*

## Abstract

Conventional aircraft wing structures consist of skins over a network of substructures and stiffeners that are approximately straight and orthogonal (ribs and spars). New manufacturing techniques such as additive manufacturing, Electron Beam Free Form Fabrication, Friction Stir Welding, and other variants have dramatically changed the cost-complexity tradeoff, and have made it worthwhile to consider the case where the underlying structure is not made of straight, regular members. The introduction of curvilinear spars and ribs (SpaRibs) has the potential to significantly increase performance, especially where the possibility of a fine tailoring of stiffness axes is beneficial, such as buckling and aeroelasticity. This paper describes a set of tools and techniques for defining, modeling, analyzing, and optimizing aircraft structures with SpaRibs, and begins to investigate the resulting performance benefits.

## Nomenclature

CG	= Center of Gravity
CRM	= Common Research Model
EBF3	= Electron Beam Free Form Fabrication
EBF3GLWingOpt	= Software for generating SpaRibs
FSW	= Friction Stir Welding
RapidFEM	= Software for generating SpaRibs
Sparib-Morph	= Software for generating SpaRibs
MTOGW	= Maximum takeoff gross weight
NASA	= National Aeronautics and Space Administration
Sparib	= Curvilinear Ribs and Spars
$I_{ij}$	= Moment of Inertia
$P_i$	= Penalty for Optimization
$V_{\text{flutter}}$	= Flutter Speed
$W_i$	= Weighting Factors for Optimization
$m$	= Wing Mass
$m_0$	= Baseline Wing Mass

<sup>1</sup> Staff Engineers, M4 Engineering, Inc.

<sup>2</sup> Chief Engineer, M4 Engineering, Inc., Associate Fellow AIAA

<sup>3</sup> Graduate Research Associate, Department of Biomedical Engineering and Mechanics

<sup>4</sup> Postdoctoral Fellow, Department of Aerospace and Ocean Engineering

<sup>5</sup> Mitchell Professor of Aerospace and Ocean Engineering, Affiliate Professor, Engineering Science and Mechanics, Associate Fellow AIAA

<sup>6</sup> Senior Aerospace Engineer, Aerostructures Branch, Senior Member AIAA

## I. Introduction

Classical structural design of aircraft wing boxes uses components such as straight spars, straight ribs, and quadrilateral wing skin panels with straight stiffeners. The components are typically connected by fastening or bonding, making the use of straight, or nearly straight internal structure a manufacturing requirement. A new design philosophy, using curvilinear stiffening members (SpaRibs and stiffeners), pioneered by Kapadia and his group at Virginia Tech<sup>1,2,3,4,5</sup>, has been introduced based on emerging manufacturing technologies such as Electron Beam Free Form Fabrication (EBF3)<sup>6</sup> and Friction Stir Welding (FSW)<sup>7</sup>.

Using these innovative technologies, the wing structure is manufactured as an integrated part instead of using mechanically fastened structural components. Compared to the conventional straight spars and ribs, the curved SpaRibs have the advantage of coupling between bending and torsional rigidity. Also, the curvilinear stiffeners have shown potential in improving the buckling resistance of local panels<sup>8,9,10</sup>. The concept of curved stiffening members enlarges the design space and leads to the possibility of a more efficient aircraft design.

The goal of the following research is to demonstrate the advantage of using curvilinear spars and ribs (SpaRibs) for the structural design of aircraft wing structures. Previous research has demonstrated the potential of utilizing SpaRibs for structural optimization of a single wing section considering strength and flutter constraints. Ongoing research aims to extend this concept to the full wing structure. The NASA Common Research Model (CRM) was used as the basis for the wing structure.

The topology of the wing structure is optimized using SpaRibs with considerations for strength, flutter, and panel buckling. An overview of the optimization process can be seen in Figure 1. The framework for the optimization is essentially a nested optimization process with two levels. The upper level optimizer controls the topology variables of the configuration. This includes the number of SpaRibs, their starting and ending points, and their shape. These variables determine the shape of the configuration and are used to generate a mesh. The lower level optimizer controls the structural sizing (e.g. thickness, composite ply angles) to satisfy stress, buckling, and flutter constraints.

The process for a single topology begins with a sizing optimization for minimum weight using quasi-static flight loads (typically including a 2.5g pullup and 1g pushover maneuver). Skin and SpaRib thicknesses are varied to meet the stress constraints. The resulting FEM load conditions are then reapplied to the vehicle with an additional buckling constraint. Skin and SpaRib thicknesses are updated where necessary to satisfy buckling constraints. The loads are then updated and the buckling optimization is repeated to convergence.

Upon convergence of the stress/buckling iteration, a flutter analysis is performed to determine the flutter speed. The flutter analysis can optionally include aeroservoelastic control laws, and a further optimization to satisfy flutter constraints can be introduced at this step, although this is not a focus of the current results. In the context of an aircraft design, the objective function would typically be to minimize the weight, possibly with penalties associated with failing to satisfy some other design constraints. In our case, we are evaluating the aeroelastic benefit of the SpaRib technologies, so our objective is to optimize the topology such that we get the highest possible flutter speed, subject to being no heavier than a baseline configuration (with conventional rib/spar internal structure). In this case, we construct a composite objective function:

$$F = \frac{1}{V_{flutter}} + W_{mass} P_{mass}$$
$$P_{mass} = \max(0, m - m_0)$$

Where  $F$  is the objective to minimize,  $W_i$  are the weighting factors,  $P_{mass}$  is the mass penalty,  $m$  is the wing mass,  $m_0$  is the baseline wing mass, and  $V_{flutter}$  is the flutter speed. The mass penalty ensures that designs with more mass than the baseline are penalized. It is assumed that the sizing optimization loop results in designs where the stress and buckling constraints are satisfied, and stress/buckling problems are reflected in a high structural weight.

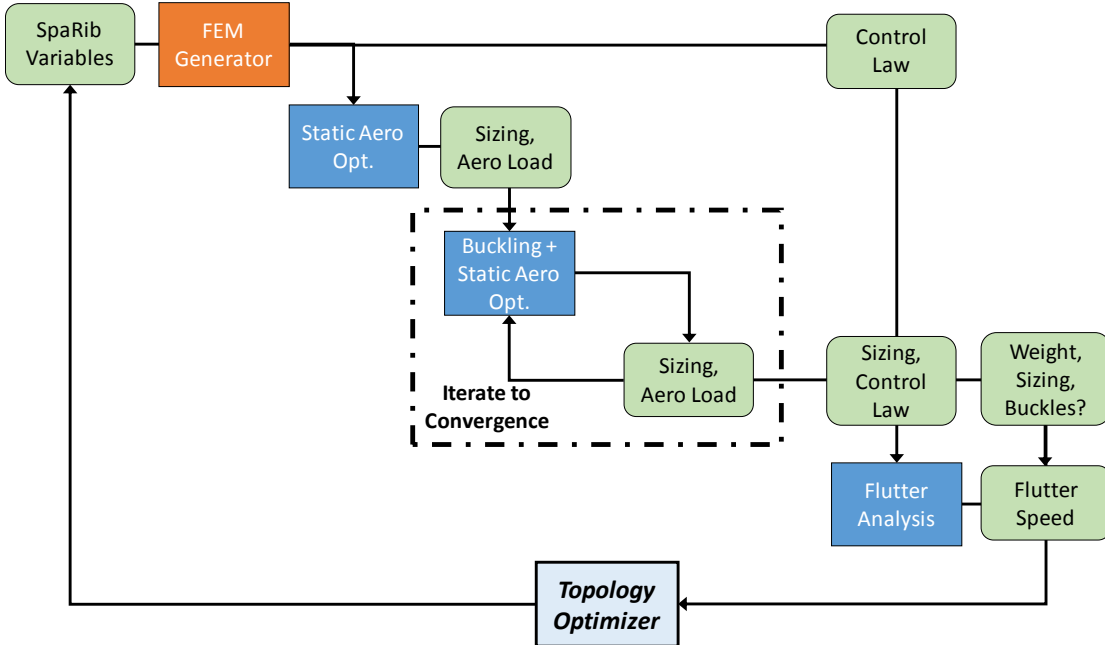


**Figure 1: Optimization process overview**

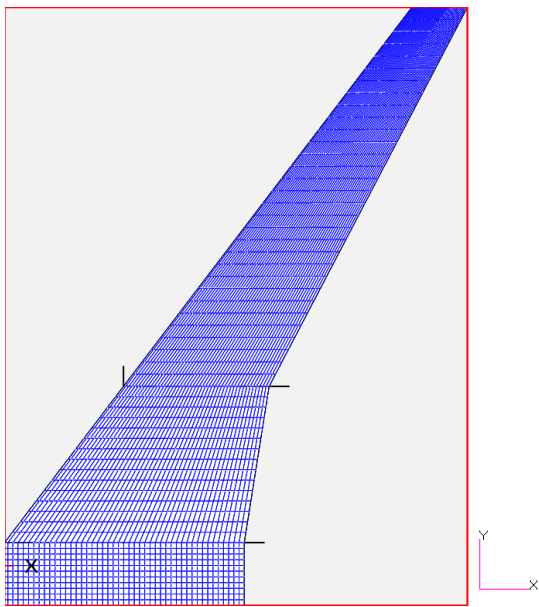
## II. SpaRib Parameterization Methods

In order to address the different scenarios in which SpaRibs may be used in aircraft optimization, a family of modeling and optimization tools have been developed:

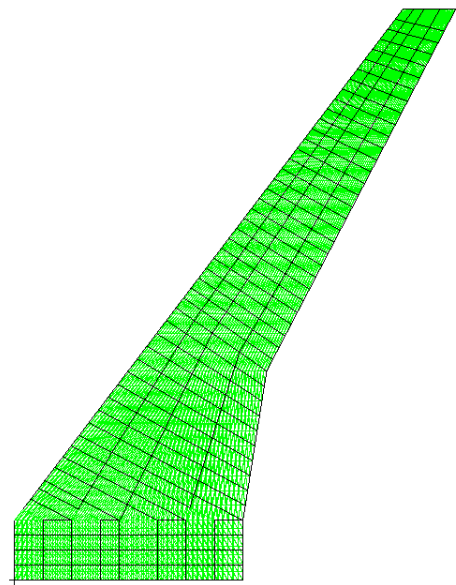
- EBF3GLWingOpt directly constructs the geometric surfaces representing SpaRibs, and meshes them in a commercial FEA preprocessing package, and has the associated advantages.
- SpaRib-Morph updates an existing finite element model by modifying the internal structure, making it useful in cases when small changes to an existing configuration are desired.
- RapidFEM is a toolset that constructs an aeroelastic model (e.g. flaps, hinge stiffness, aero panels) directly from outer mold line geometry and a 2D “sketch” describing the internal structure.

These different approaches provide a toolkit for optimizing SpaRib configurations in different environments and different constraints. Since the results models and results presented here were developed with the RapidFEM approach, this will be discussed in some detail below. For details on the other approaches, EBF3GLWingOpt is discussed in references 2 and 3, while SpaRib-Morph is discussed in reference 11.

RapidFEM<sup>12</sup> is a software program developed to automatically generate geometry and finite element models of complex built-up structures for rapid concept evaluation and structural optimization. In this process, top-level geometry in a simplified format is provided to the RapidFEM program along with information about the structural layout. The required geometric operations are then performed to divide the surface into numerous patches, each of which represents a single structural component, which are then used to mesh the geometry. This process has been used to develop the baseline ASE models for the CRM-derived configuration as shown in Figure 2 and Figure 3.



OML Constructed  
in OpenVSP



- Sketch is defined in dihedral plane
- RapidFEM handles projection/  
intersection and meshing

Figure 2: Outer Mold Line and 2D Sketch of the CRM-derived configuration.

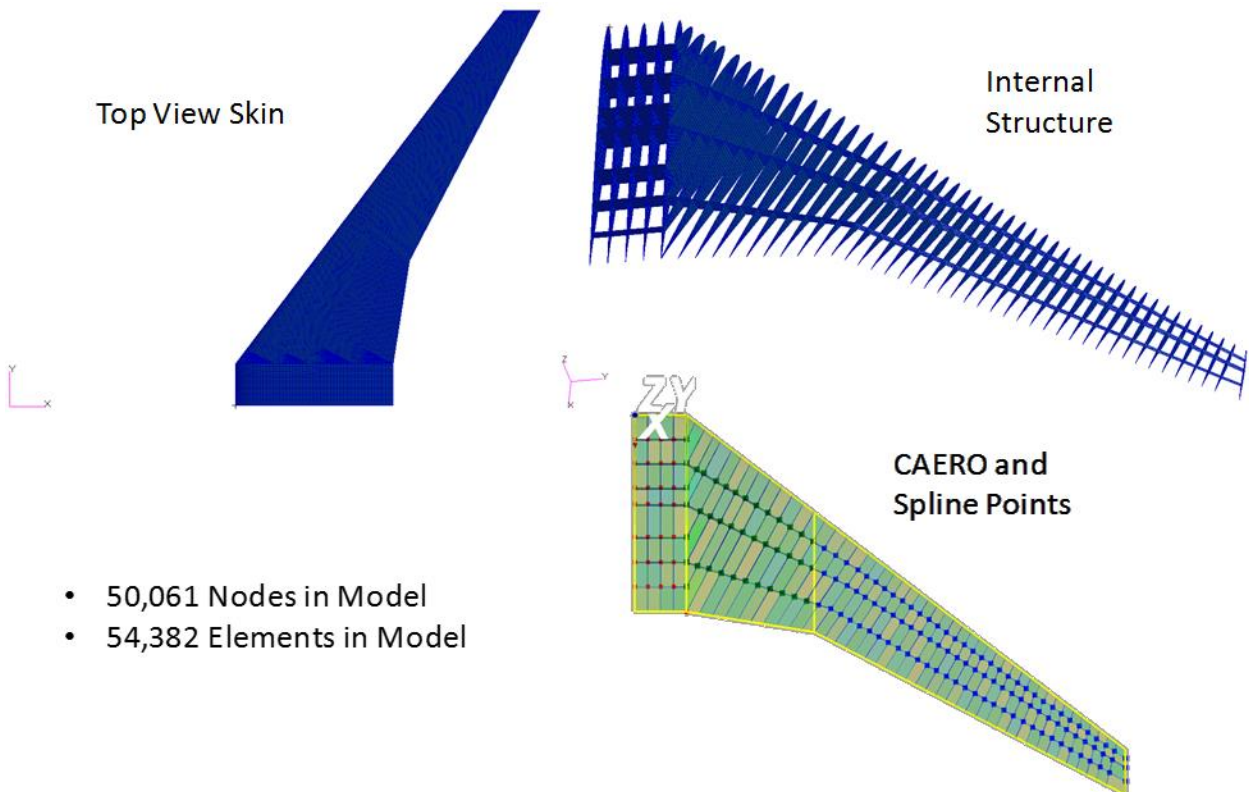
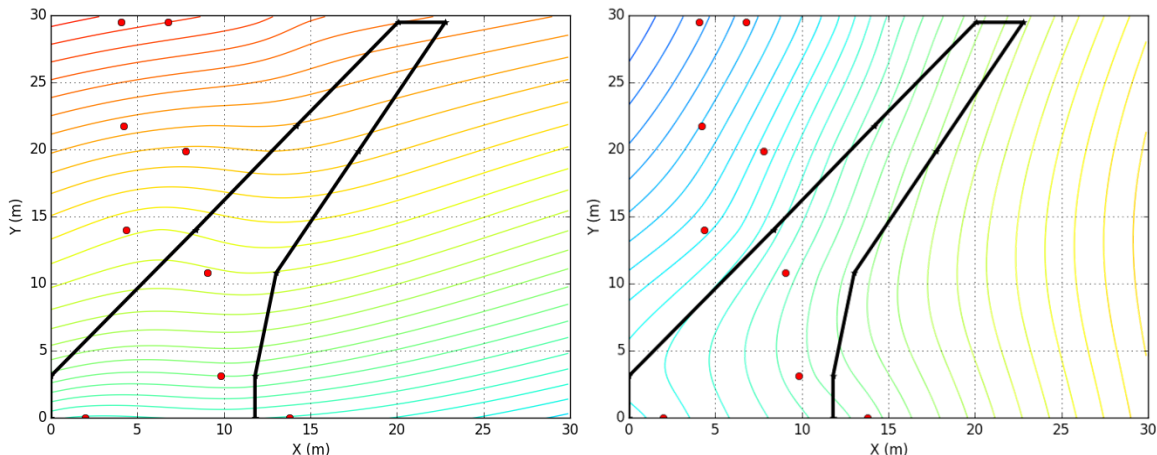


Figure 3: Resulting structural and aerodynamic models for ASE analysis.

In the context of this paper, RapidFEM has been applied to generate SpaRib internal structures by approximating each curvilinear SpaRib with a piecewise linear approximation (straight sections within one bay). In order to accomplish this, a method of parameterizing the internal structural layout has been developed based on generating functions. In this approach, a function in the dihedral plane of the wing for each set of structural members is defined. In the normal context of ribs and spars (or rib-like SpaRibs and spar-like SpaRibs), this would be one function for the spars, and one for the ribs. A series of contour levels for each of these functions at which structural members will be placed is defined. A rib is created along each contour of the rib function, and a spar along each contour of the spar function. This is shown notionally in Figure 4. Note that the functional form of these functions is arbitrary, so long as they support parameters that can capture the desired range of rib/spar configurations.

A preprocessor routine processes constructs a RapidFEM sketch based on the generating functions, the wing boundary, and the rib and spar contour levels. We have found that a wide variety of internal structural configurations can be obtained with relatively few configuration design variables. It is expected that through the use of design variable linking, and families of C0 and C1 continuous functions (e.g. finite element shape functions) this can be further reduced, and handle many of the practical issues of aircraft internal structure.



**Figure 4: Contours of the generating function for spar-like and rib-like SpaRibs.**

### III. Baseline Transport Configuration

The demonstration problem for the SpaRib optimization process is a representative commercial transonic passenger aircraft configuration.

#### A. NASA Common Research Model

The NASA Common Research Model project provides a standardized model for comparison of computational fluid dynamic codes with experimental data<sup>13</sup>. A digital surface model based on the Boeing 777-200 was created. A scale model was built and tested in the NASA National Transonic Facility. For the current research, the wing surface model of the CRM was used to define the geometry of the wing structure and of the aerodynamic model<sup>14</sup>.

#### B. Wing Structural Model

The baseline structural model this study is constructed by intersecting the 2D sketch with the outer mold line of the vehicle to construct individual rib, spar, and skin panels. In the baseline case, the ribs and spars are straight, and approximate the internal structural layout of a conventional transport aircraft wing. The wing mesh seen in Figure 5 is comprised of shell elements that make up the ribs, spars, and skins, and will form the baseline which will be compared to topology-optimized configurations with SpaRibs.

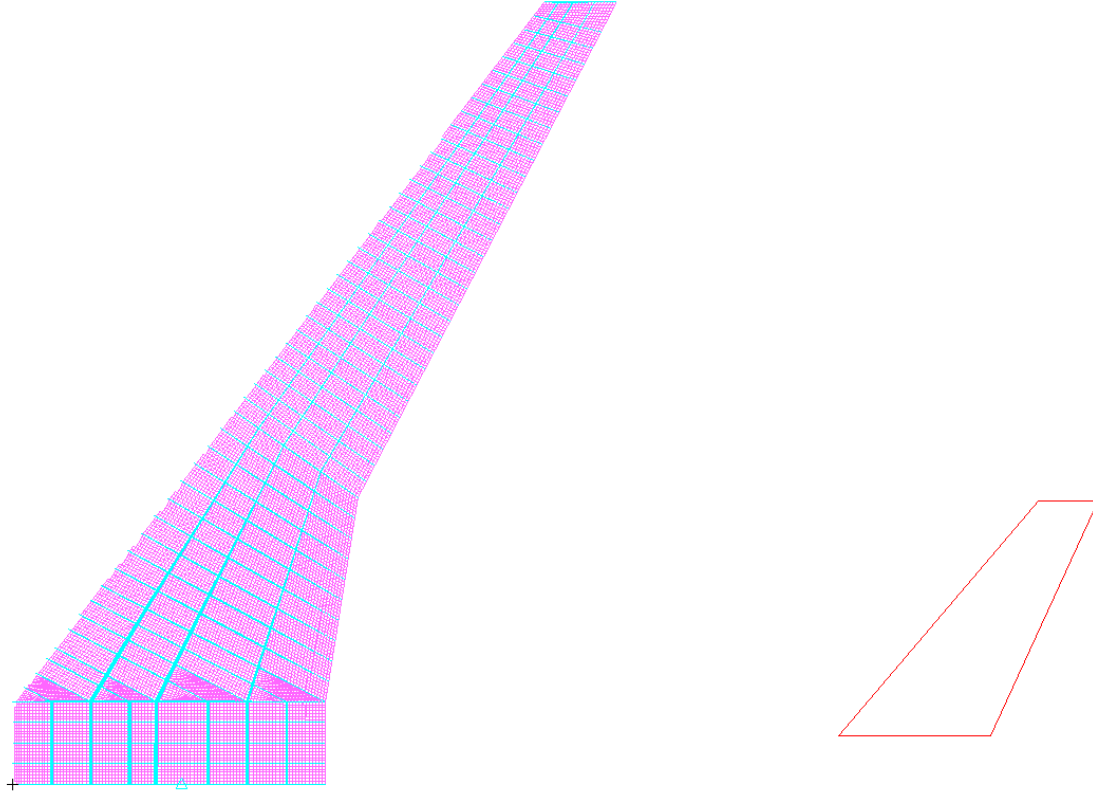


**Figure 5: Baseline model created by RapidFEM. Note that rigid body fuselage/tail model was used for simplicity.**

### C. Vehicle Aero and Mass Model

As the NASA CRM was based on the Boeing 777-200, it was used as the basis for the aerodynamic and mass models. Figure 6 shows a side view of the aircraft and the reference marker.

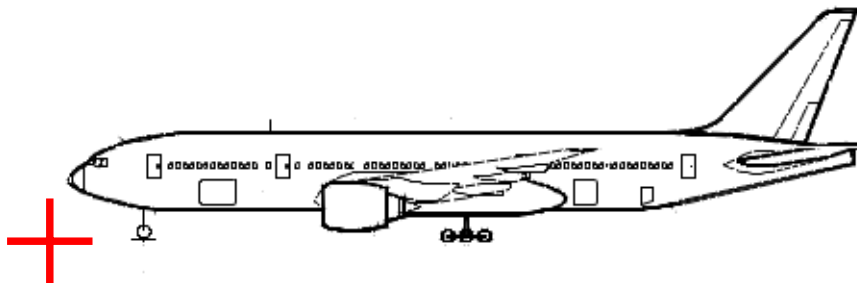


**Figure 6: B777-200 Side view with origin marker 15.**

#### C.1. Aerodynamic Model

In order to analyze static and dynamic aeroelastic responses, a vehicle aerodynamic model was created. The model was created using the Doublet Lattice Method<sup>16</sup>. Aerodynamic panels were created for the wings and horizontal stabilizers. The dimensions for these panels were extracted from the full body CRM .iges models<sup>14</sup>. The doublet lattice panels for the wing, along with associated spline and camber data, were generated automatically by RapidFEM (see Figure 8 and Figure 9).

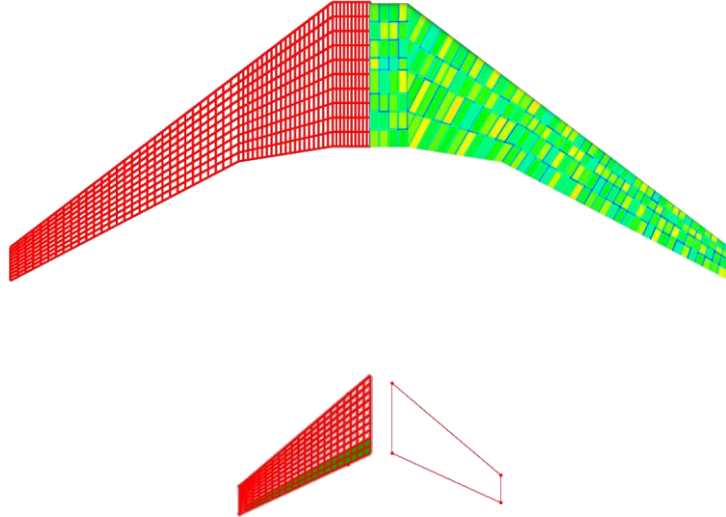


**Figure 7: Vehicle finite element model and doublet lattice subpanels.**

Aerodynamic control surfaces were created to allow for trimmed maneuver analysis. Since the focus here is on structural sizing with symmetric maneuvers, only the horizontal tail with elevators were modeled. Dimensions of the control surfaces were extracted from scale drawings of the B777-200 from the airport planning document<sup>15</sup>. No structural models of control surfaces or hinge mechanisms were included in the FEM for this portion of the effort.

To account for twist and camber of the wing airfoil, a downwash correction was used. For each spanwise row of doublet-lattice subpanels, an airfoil was extracted from a fine mesh of the wing outer mold line (OML). From each airfoil, a camber line spline was generated. Figure 8 shows a few example airfoils and camber lines using this method. The camber spline was discretized at each chordwise subpanel and the incidence angle was computed. The structural and aerodynamic models were connected to one another using a surface spline methodology. The spline points used for this interconnection are shown in Figure 9.

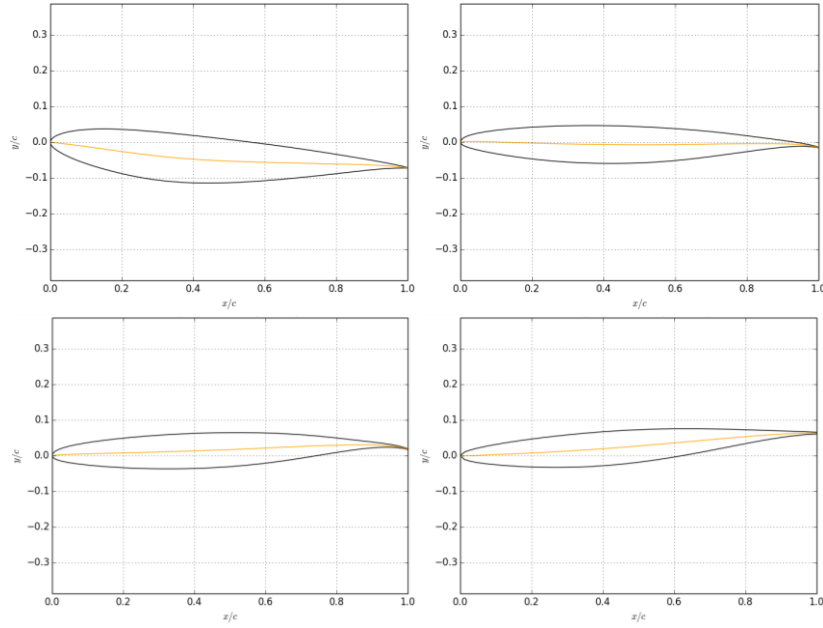


**Figure 8: Airfoils and camber lines at root, 37% span, 50% span, and tip.**

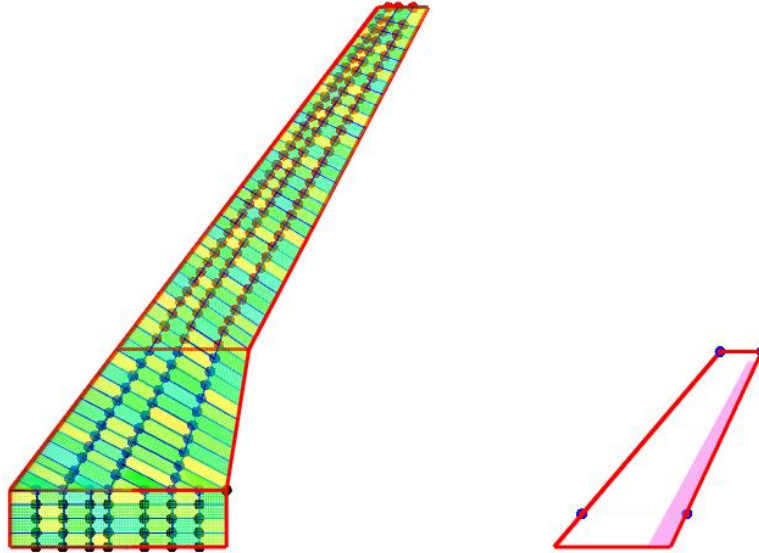


**Figure 9: Spline points used to connect structural and aerodynamic models.**

### C.2. Mass Model

The mass properties of the model were determined to match the B777-200 in the maximum takeoff gross weight (MTOGW) configuration. The mass of the aircraft at MTOGW is 545,000 lb. Nonstructural mass was added to the wing to represent fuel, control surfaces, mechanisms, and other components not modeled in the finite element model. In order to match the total vehicle, a point mass was added to the model with mass equal to the MTOGW mass less the wing structural mass, at a location to give the most forward CG (typically critical for wing sizing).

The aircraft moments of inertia are needed for flutter analysis. Due to a lack of published data, moments of inertia were estimated using the technique of Roskam<sup>17</sup>. The non-dimensional radii of gyration from the B737-200 were used to estimate  $I_{xx}$ ,  $I_{yy}$ , and  $I_{zz}$  for the 777-200 aircraft.  $I_{xy}$ ,  $I_{xz}$ , and  $I_{yz}$  were neglected as only the wing was of interest. The moments of inertia less the contributions from the wing structure were applied at the point mass.

The aircraft center of gravity was also estimated. The  $y$  (spanwise) location was assumed to lie along the aircraft centerline. The  $x$  (chordwise) location was determined from the landing gear loading chart and the landing gear geometry. The loading was taken for the 93.8% main gear loading condition. The  $z$  location was estimated as 25% of the fuselage height. The location of the point mass was positioned such that the overall model CG matched these estimates. Note that as of this time, neither landing nor taxi load cases have been included. Table 1 lists a summary of the mass properties.

**Table 1: Aircraft mass properties (excluding wing).**

Parameter	Units	Value
Mass	lb	482,000
$I_{xx}$	lb ft <sup>2</sup>	1.81e8
$I_{yy}$	lb ft <sup>2</sup>	1.13e8
$I_{zz}$	lb ft <sup>2</sup>	3.08e8
$I_{xy}$	lb ft <sup>2</sup>	0
$I_{xz}$	lb ft <sup>2</sup>	0
$I_{yz}$	lb ft <sup>2</sup>	0
$CG_x$	ft	98.95
$CG_y$	ft	0
$CG_z$	ft	11.65

### C.3. Vehicle Model

In order to take advantage of symmetry in the analysis process, a half-aircraft model was constructed. The vehicle model includes a single (starboard) wing shell model, the associated mass and aerodynamic components, a concentrated mass to represent the fuselage, cargo, and fuselage fuel, and rigid, massless elements to model the fuselage and tail. Figure 7 shows a top view of the vehicle half model including the shell mesh (colored by node id) and mass-less bar elements to aid in visualizing the tail. The aerodynamic sub-panels (in red) and tail control surface (in green) are shown on the left half plane for visualization, but are located on the right half of the model.

### D. Sizing Optimization

A sizing optimization on skin, spar, and rib thickness is performed, with the objective of minimizing mass subject to stress and buckling constraints. Each skin, spar, and rib thickness is a variable. This analysis is performed relative to a set of specified load conditions which include a 2.5g pull-up maneuver, a 1.0g push-over maneuver, and (optionally), additional flight and static cases.

### E. Aeroelastic Analysis

The 2.5g pull-up maneuver linear analysis results are shown below in Figure 10. For this maneuver, the wingtip deflection is 244", and it is clear that the stress in each design region approaches the 50 ksi allowable, other than in areas such as the leading and trailing edges that are not intended to carry main wing bending loads, and are not sized by the trim load cases. Note that the 244" deflection is relatively large and that as of yet, no geometric nonlinearity has been considered. In the future, a deflection constraint may be added to force the deflections to lie within the geometrically linear range.

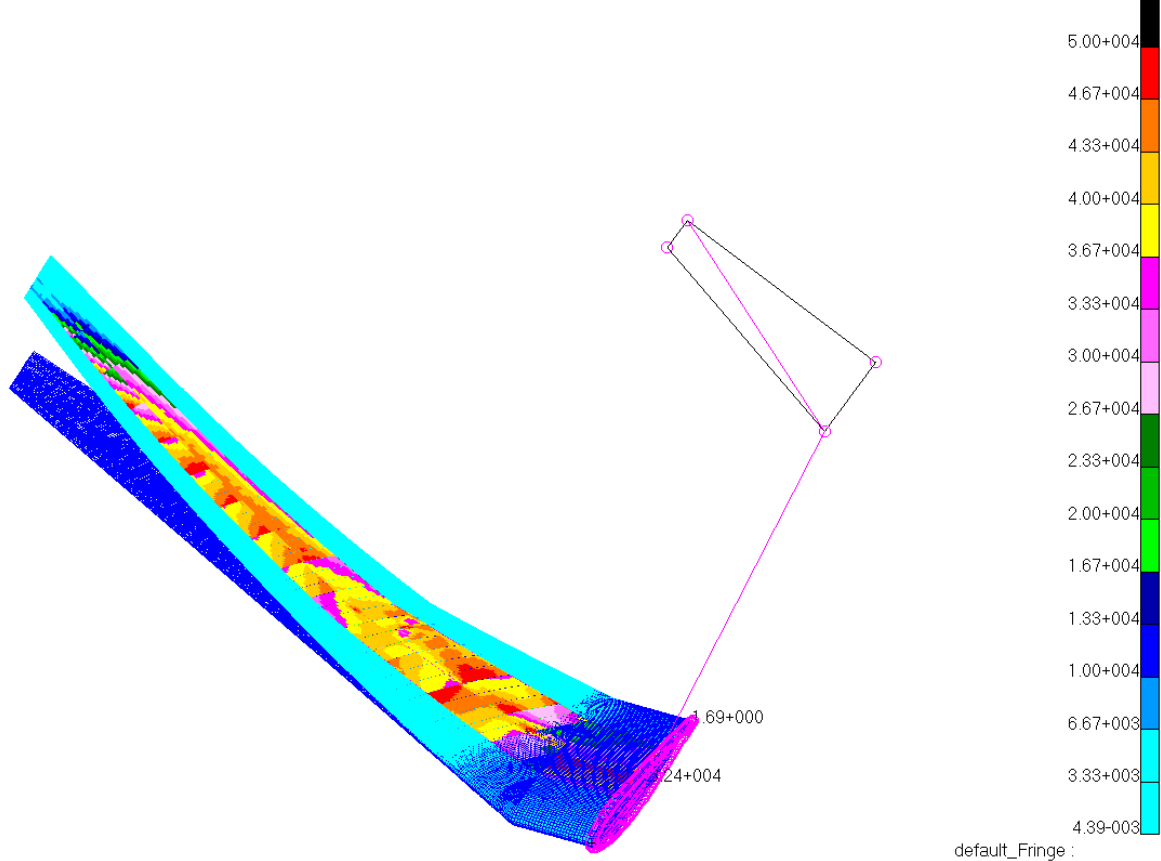
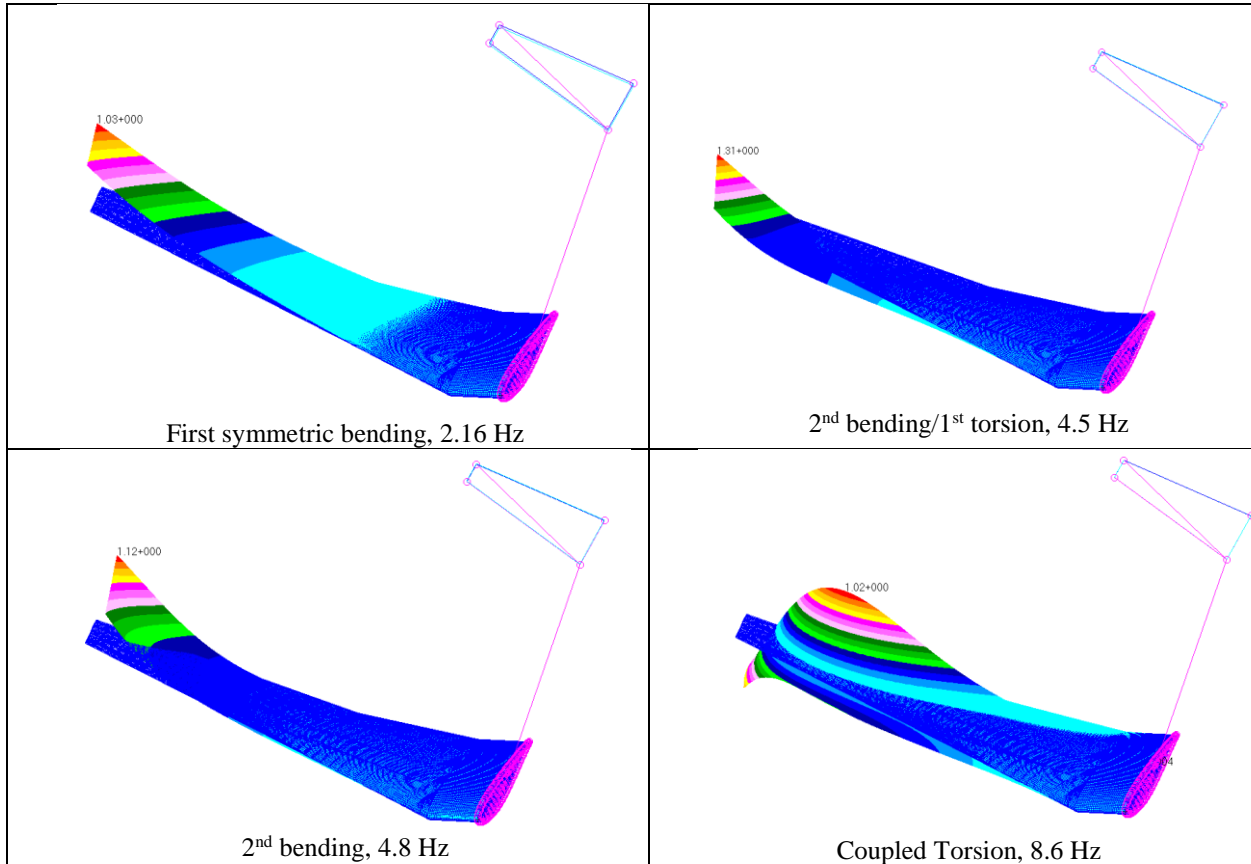
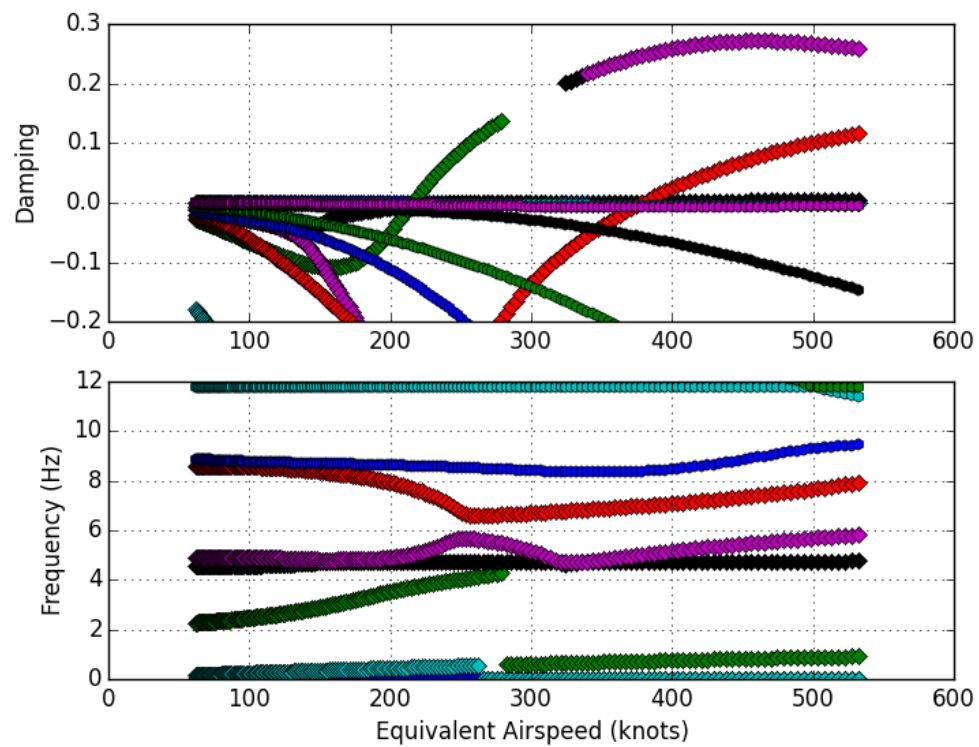


Figure 10: 2.5g pull-up maneuver.

The important structural modes are shown in Figure 11. This configuration shows flutter interactions involving the first bending mode, the 2nd bending/1st torsion mode, and the coupled torsion mode, as shown in the V-g plots in Figure 12. Note that for this configuration, the flutter speed is relatively low as no flutter constraint was applied during the optimization. However, different internal structural arrangements, either to increase torsional stiffness or change the bend/twist coupling, are expected to provide part of the solution, and reduce the resulting flutter penalty. Also note that the lack of consideration for flutter during this phase of the design optimization was intentional as the objective is to maximize flutter speed with no change in structural weight. The aeroelastic mode shapes for the primary flutter modes are shown in Figure 13 and Figure 14.



**Figure 11: Important Symmetric Structural Modes.**



**Figure 12: Aeroelastic Analysis Results at Mach 0.9.**

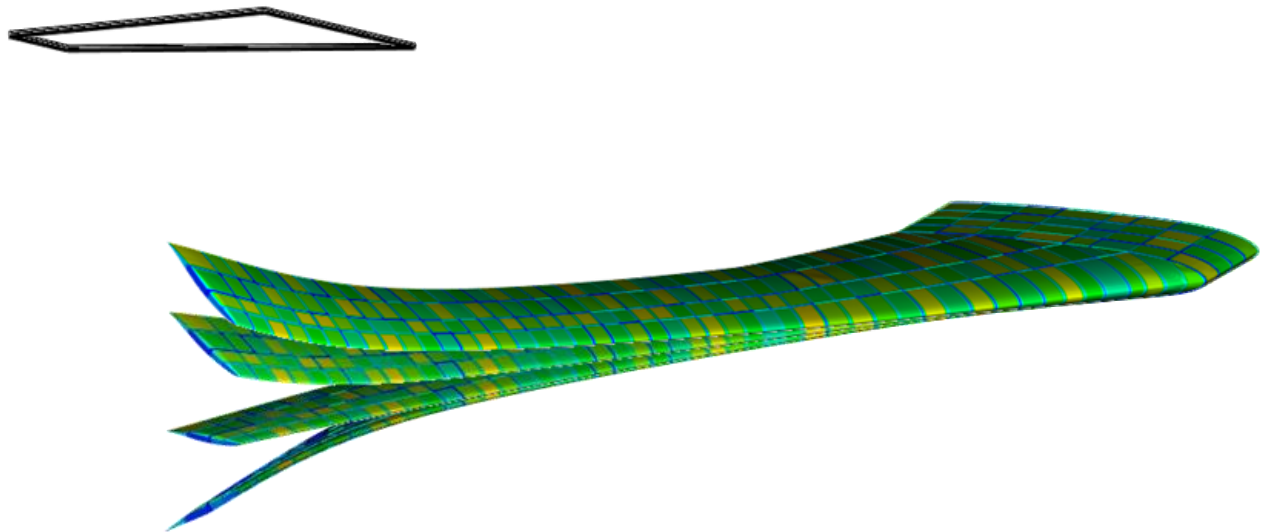


**Figure 13: Primary Flutter Mode (216 knots).**



**Figure 14: Secondary Flutter Mode (379 knots).**

#### IV. SpaRib Configurations

A family of SpaRib configurations has been defined based on 17 design variables. The first 8 design variables define the rib potential function (the number, placement, curvature, and orientation of the ribs), and the last 9 design variables define the spar potential function (the number, placement, curvature, and orientation of the spars). This results in a 17-variable description of many possible combinations of ribs and spars, without a priori assumptions about the topology. Two such configurations are shown below, one with the spars swept slightly forward, and another with the spars swept slightly aft. The RapidFEM sketches for these two configurations are shown Figure 15.

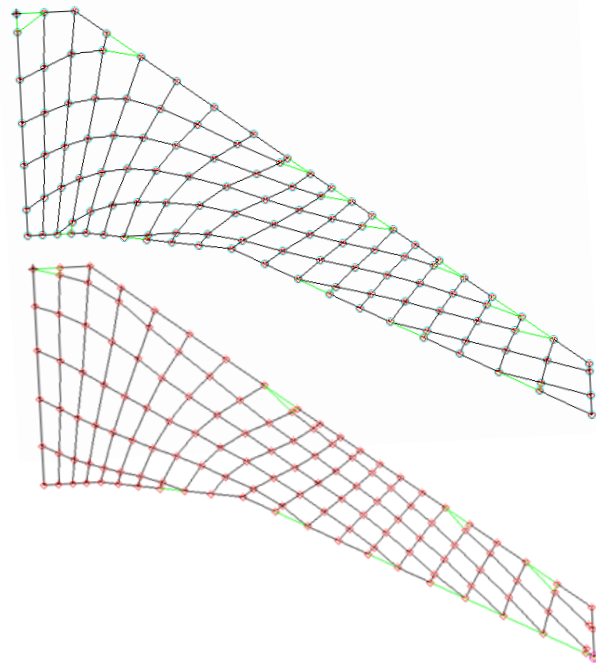


**Figure 15: RapidFEM sketches for forward (top) and aft (bottom) swept SpaRib configurations.**

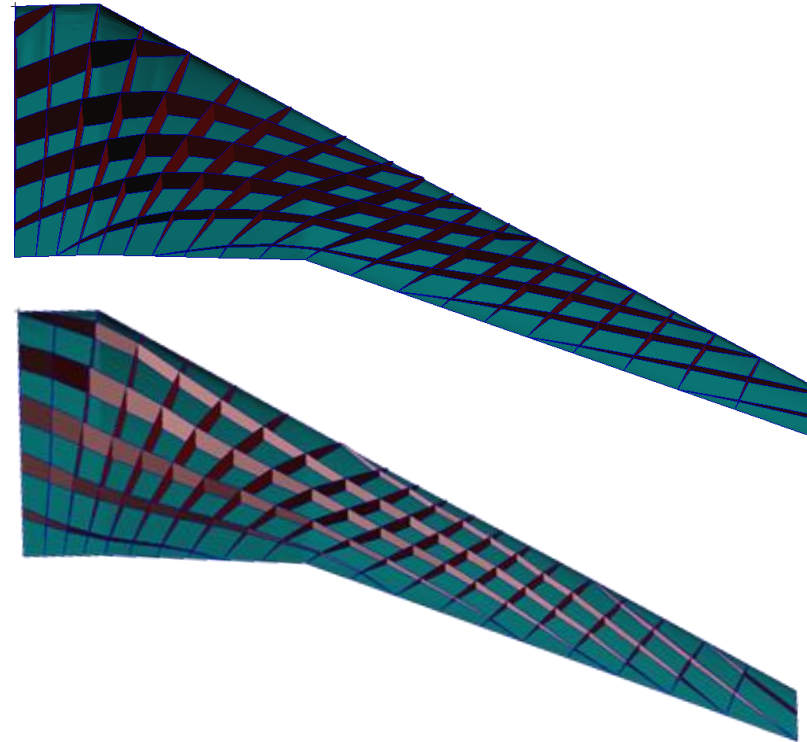


**Figure 16: Isometric view of structural meshes for forward (top) and aft (bottom) swept SpaRib configurations (only free patch edges are shown).**

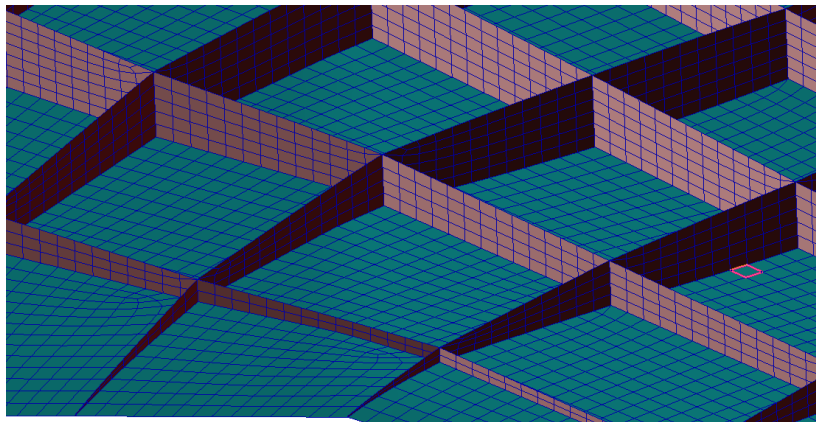


**Figure 17: Close-up of the wing break region for the aft swept spar.**

The resulting structural finite element models are shown in Figure 16 and Figure 17. These two configurations were selected as the first SpaRib configurations because the spar sweeping of the internal structure is expected to directly impact the bend-twist coupling of the wing, and therefore the aeroelastic behavior. The rib sweeping between the two configuration was held constant. Complete aeroelastic models of these configurations have been constructed, and analysis/optimization is underway and will be presented in a future publication.

## V. Conclusion / Future Work

The use of curvilinear internal structure arranged in non-conventional ways is enabled by new manufacturing technology. As these new manufacturing approaches mature, the cost-complexity tradeoff of aerospace structures will completely change, making previously unlikely structural layouts possible. In this paper we have presented a set of approaches for defining, modeling, analyzing, and optimizing aircraft structures using this new paradigm. This “opening of the design space” has the potential to lead to revolutionary structural concepts and configurations that may have improved performance over conventional rib/spar configurations.

In future work, a complete optimization of the baseline configuration including strength, buckling, wing tip deflection, and flutter analysis will be considered. The baseline optimized configuration (with straight spars and ribs) presented in this paper will be the baseline, after which the SpaRib configuration variables will be optimized to provide a combination of reduced weight and/or increased flutter speed. A flutter suppression control system design will be added to demonstrate the possible weight savings of an aeroservoelastically optimized SpaRib configuration.

## VI. Acknowledgment

This effort was funded by the NASA SBIR/STTR program, under contracts NNX14CD16P and NNX15CD08C.

## VII. References

- <sup>1</sup>Locatelli, D., Mulani, S. B. and Kapania, R. K. "Wing-Box Weight Optimization Using Curvilinear Spars and Ribs (SpaRibs)," Vol. 48, No. 5, September-October 2011, pp. 1671-1684.
- <sup>2</sup>Liu, Q., et al. "Global/Local Optimization of Aircraft Wing Using Parallel Processing," *Journal of Aircraft*, 2016.
- <sup>3</sup>Locatelli, D., et al. "Multidisciplinary Optimization of Supersonic Wing Structures Using Curvilinear Spars and Ribs (SpaRibs)," *54th AIAA/ASME/ASCE/AHS/ASC Structures, Structural Dynamics, and Materials Conference, Structures, Structural Dynamics, and Materials and Co-located Conferences*, AIAA 2013-1931, Boston, Massachusetts, 2013.
- <sup>4</sup>Dubois, A., Farhat, C. and Abukhwejah, A H. "Parameterization Framework for Aeroelastic Design Optimization of Bio-Inspired Wing Structural Layouts," *57th AIAA/ASCE/AHS/ASC Structures, Structural Dynamics, and Materials Conference*, AIAA 2016-0485, San Diego, California, USA, 4-8 January 2016.
- <sup>5</sup>Jutte, C. V., Stanford, B. K. and Wieseman, C. D. *Internal Structural Design of the Common, Research Model Wing Box for Aeroelastic Tailoring*, Hampton, VA : Nasa Report, 2015. NASA/TM-2015-218697
- <sup>6</sup>Taminger, K. M. B. and Hafley, R A. "Electron Beam Freeform Fabrication: A Rapid Metal Deposition Process," *Proceedings of 3rd Annual Automotive Composites Conference*, MI. Society of Plastics Engineers, Troy, 2003.
- <sup>7</sup>Nicholas, E. D. "Developments in the Friction-Stir Welding of Metals," *ICAA-6: 6th International Conference on Aluminium Alloys*, 1998.
- <sup>8</sup>Mulani, S. B., Slemp, W. C. and Kapania, R. K. "EBF3PanelOpt: An Optimization Framework for Curvilinear Blade-Stiffened Panels," Vol. 63, 2013, pp. 13-26.
- <sup>9</sup>Jrad, M., Mulani, S. B. and Kapania, R. K. "A Framework for Damage Tolerance and Optimization of Stiffened Panels," *International workshop on structural health monitoring*, Stanford University, Stanford, CA, 1-3 September 2015.

<sup>10</sup>Jrad, M., Khan, A. and Kapania, R. K. "Buckling Analysis of Curvilinearly Stiffened Composite Panels with Cracks," *55th AIAA/ASME/ASCE/AHS/ASC Structures, Structural Dynamics, and Materials Conference*, Maryland, National Harbor, 13-17 January 2014, 2014.

<sup>11</sup>M4 Engineering, Inc, *SpaRib-Morph User's Manual*, Long Beach, CA : M4 Engineering, Inc., 2015.

<sup>12</sup>M4 Engineering, Inc. , *RapidFEM User Manual, Version 5.0.0*, Long Beach, CA 90807 : M4 Engineering, Inc., October 2015.

<sup>13</sup>Vassberg, John C., et al. *Development of a Common Research Model for Applied CFD Validation Studies*, s.l. : AIAA, 2008.

<sup>14</sup> NASA Common Research Model, [Online] May 21, 2013. [Cited: September 3, 2015.] <http://commonresearchmodel.larc.nasa.gov/iges-files/>,

<sup>15</sup>Boeing, *777-200/300: Airport Characteristics for Airport Planning*, Boeing Commercial Airplanes, Seattle, 2011.

<sup>16</sup>MSC Software Corporation, "MSC Nastran Aeroelastic Analysis User's Guide," Santa Ana, CA, 2004.

<sup>17</sup>Roskam, Jan, *Airplane Design Part V: Component Weight Estimation*, University of Kansas, Ottawa, Kansas, 1989.